

The non-coding *Air* RNA is required for silencing autosomal imprinted genes

Frank Sleutels*, Ronald Zwart* & Denise P. Barlow†

* Department of Molecular Genetics, The Netherlands Cancer Institute, Plesmanlaan 121, 1066CX, Amsterdam, The Netherlands

† ÖAW Institute of Molecular Biology, Billrothstrasse 11, A5020 Salzburg, Austria

In genomic imprinting, one of the two parental alleles of an autosomal gene is silenced epigenetically by a *cis*-acting mechanism^{1,2}. A bidirectional silencer for a 400-kilobase region that contains three imprinted, maternally expressed protein-coding genes (*Igf2r/Slc22a2/Slc22a3*) has been shown by targeted deletion to be located in a sequence of 3.7 kilobases^{3–5}, which also contains the promoter for the imprinted, paternally expressed non-coding *Air* RNA⁶. Expression of *Air* is correlated with repression of all three genes on the paternal allele⁵; however, *Air* RNA overlaps just one of these genes in an antisense orientation⁶. Here we show, by inserting a polyadenylation signal that truncates 96% of the RNA transcript, that *Air* RNA is required for silencing. The truncated *Air* allele maintains imprinted expression and methylation of the *Air* promoter, but shows complete loss of silencing of the *Igf2r/Slc22a2/Slc22a3* gene cluster on the paternal chromosome. Our results indicate that non-coding RNAs have an active role in genomic imprinting.

Most mammalian imprinted genes are found in clusters that also contain imprinted non-coding RNAs^{2,7}. In many cases, expression of the non-coding RNA from one parental allele correlates with repression of linked protein-coding genes on the same allele, raising the possibility that non-coding RNAs either are required for silencing or are a consequence of the silencing mechanism. Studies

of the *Igf2/Ins2/H19* imprinted gene cluster on mouse chromosome 7 have shown, however, that the *H19* non-coding RNA does not have a role in silencing the *Igf2/Ins2* protein-coding genes^{8,9}. Instead, imprinted expression of *Igf2/Ins2* occurs through a silencer element¹⁰ and an insulator element (called *H19*-DMR) close to the *H19* promoter, and imprinted expression of *H19* is thought to occur as a consequence of paternal-specific methylation of the insulator element^{11,12}. Thus, despite the prevalence of imprinted autosomal non-coding RNAs, none has been shown to be required for the silencing of flanking imprinted protein-coding genes.

We have studied the paternal-specific *Air* non-coding RNA on mouse chromosome 17 that is expressed from a promoter located in intron 2 of the *Igf2r* gene. This non-coding RNA is 108 kilobases (kb), polyadenylated but apparently unspliced, and overlaps the *Igf2r* promoter^{3,6}. Deletion of a 3.7-kb imprint control element (ICE) that contains the *Air* promoter releases paternal-specific silencing of three genes, *Slc22a2* and *Slc22a3* that are located upstream, and *Igf2r* that is located downstream^{4,5}. Thus, the 3.7-kb ICE has a bidirectional action despite the fact that *Air* overlaps only one of these genes (ref. 5; and Fig. 1a).

To test whether imprinted expression of the *Air* RNA is required for silencing, we truncated *Air* to 4% of its length by inserting a 1.2-kb polyadenylation cassette into the β -globin gene at the downstream border of the 3.7-kb ICE to yield the *Air-T* allele (Fig. 1). The modification was designed to truncate *Air* without disrupting the function of the 3.7-kb ICE, as assessed by its ability to attract a maternal-specific methylation imprint and to show paternal-specific expression of the *Air* promoter^{3,6}. Mice with a maternally inherited *Air-T* allele (*Air-T*/+), note that the maternal allele precedes the paternal one in all genotypes shown here) were identical to wild type, whereas mice with a paternally inherited *Air-T* allele (+/*Air-T*) and homozygous *Air-T* mice showed a 15% reduction in birth weight as compared with wild-type littermates (data not shown). A similar phenotype caused by biallelic expression of *Igf2r* is seen in mice with a paternally inherited deletion of the 3.7-kb ICE; these mice do not express *Air* owing to

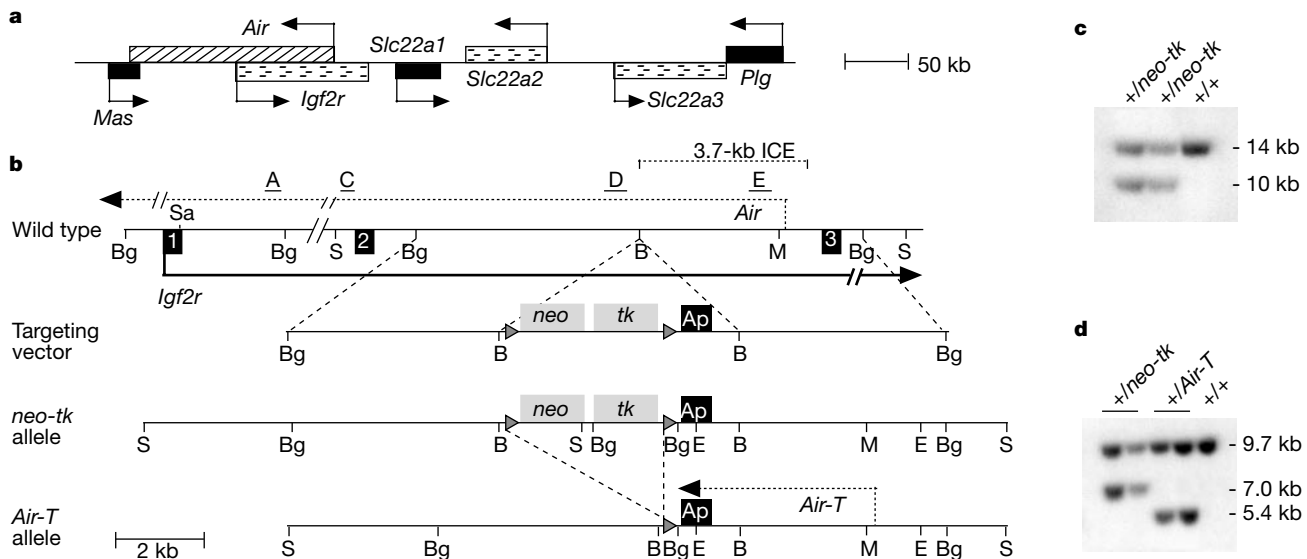


Figure 1 Generation of the *Air-T* allele. **a**, Map spanning the 400-kb imprinted cluster. Indicated are paternally expressed *Air* (hatched box), maternally expressed *Igf2r*, *Slc22a2* and *Slc22a3* (dotted boxes) and non-imprinted genes (black boxes). **b**, Wild-type allele comprises *Igf2r* (black arrow), *Igf2r* exons 1–3 (black boxes) and *Air* (dashed arrow). The locus was targeted at a *Bam*HI site bordering the 3.7-kb ICE (dotted line) that lies 3.0-kb downstream from the *Air* transcription start. The targeting vector contains a 1.2-kb rabbit β -globin gene polyadenylation cassette (Ap), and PGK–

neomycin (*neo*) and PGK–thymidine-kinase (*tk*) selection genes flanked by loxP sites (triangles). Selection genes were deleted from the *neo-tk* allele by transient Cre transfection to generate the *Air-T* allele. Probes A, C, D and E are indicated. B, *Bam*HI; Bg, *Bgl*II; E, *Eco*RI; M, *Mlu*I; Sa, *Sall*; S, *Scal*. **c**, Targeted *neo-tk* clones were identified by a 10-kb *Scal* fragment with probe C. Targeting was paternal-specific in 18 out of 18 ES clones (Supplementary Information). **d**, The *Air-T* allele was identified by a 5.4-kb *Bgl*II fragment with probe D.

deletion of the *Air* promoter⁴.

We also analysed the *Air-T* allele in reciprocal, double heterozygous crosses with mice containing a 3-cM deletion that spanned this imprinted cluster (*T^{hp}*). In a wild-type background, maternal inheritance of the *T^{hp}* allele (*T^{hp}/+*) is lethal between 15.5 and 17.5 days postcoitum (d.p.c.), owing to the absence of *Igf2r*^{4,13}. We found, however, that offspring with the *T^{hp}/Air-T* genotype were normal sized, viable and fertile, indicating that the maternal-specific *T^{hp}* phenotype had been rescued by the paternal *Air-T* allele (data not shown), as shown previously in crosses with a paternal 3.7-kb ICE deletion^{4,5}. Offspring with the reciprocal genotype (*Air-T/T^{hp}*) showed similar size, viability and fertility (data not shown) to a *+/T^{hp}* genotype.

We tested that the *Air* RNA expressed from the *Air-T* allele was truncated by using an RNase protection assay (RPA) with probes positioned across the 108 kb that is spanned by the endogenous *Air* RNA⁶ (Fig. 2a). Probes downstream from the inserted polyadenylation signal detected *Air* RNA from the paternal wild-type allele but not from the paternal *Air-T* allele, indicating the absence of stable *Air* RNA downstream from the polyadenylation cassette (Fig. 2b). We tested for polyadenylation at the inserted cassette by polymerase chain reaction with reverse transcription (RT-PCR) using a poly(dT) reverse transcription primer plus the PX6R gene-specific primer (Fig. 2a). Unexpectedly, RT-PCR generated a single 314-base-pair (bp) *Air-T*-specific fragment from a spliced, polyadenylated RNA that had used a splice donor located 53-bp downstream from the principal *Air* transcription start and a splice acceptor from the inserted exon 3 of the β -globin gene (Supplementary Information). The +53-bp splice donor has been identified in a transgene study but is not normally used in the wild-type locus; however, use

of this splice donor does not correlate with the loss of imprinting of *Igf2r/Air* in transgenes^{6,14}.

We investigated the proportion of spliced/unspliced *Air-T* RNA by RPA with probes positioned between the *Air* promoter and the inserted polyadenylation cassette (Fig. 2c). Both probe G and probe J showed that 20% unspliced *Air* RNA was present from the paternal *Air-T* allele as compared with the paternal wild-type allele (Fig. 2c). Probe K (comprising the RT-PCR fragment) detected both spliced and unspliced RNAs, and confirmed that these were present at 80% and 20%, respectively. Probe L spans the inserted polyadenylation signal and extends 404-bp downstream from the ATTTAAA signal; this probe detected the same 173-bp protected fragment as found in the control LAI-313 transgene¹⁴, showing that the ATTTAAA signal is used, but not larger protected fragments (Fig. 2c). Thus, Fig. 2 shows that although the *Air-T* allele generates spliced and unspliced *Air* RNAs, these are both truncated 4.2-kb downstream from the *Air* promoter and stable RNA is not detected downstream from the polyadenylation cassette.

We tested the function of the 3.7-kb ICE in the *Air-T* allele by analysing the methylation state, imprinted expression and the expression level of the *Air* promoter in *Air-T* mice as compared with wild-type littermates. Methyl-sensitive enzymes identified methylation specific to the maternal allele on the *Air-T* promoter as found on the wild-type allele (Fig. 3a). Analysis by RPA showed imprinted, paternal-specific expression of the *Air-T* RNA as found on the wild-type allele, and also showed that the *Air-T* allele generates similar levels of stable *Air* RNA as compared with the wild-type allele (Fig. 3b). Although it is possible that insertion of the polyadenylation cassette disturbed an as yet unidentified imprinting element or altered transcription/stability of the *Air-T* RNA, the

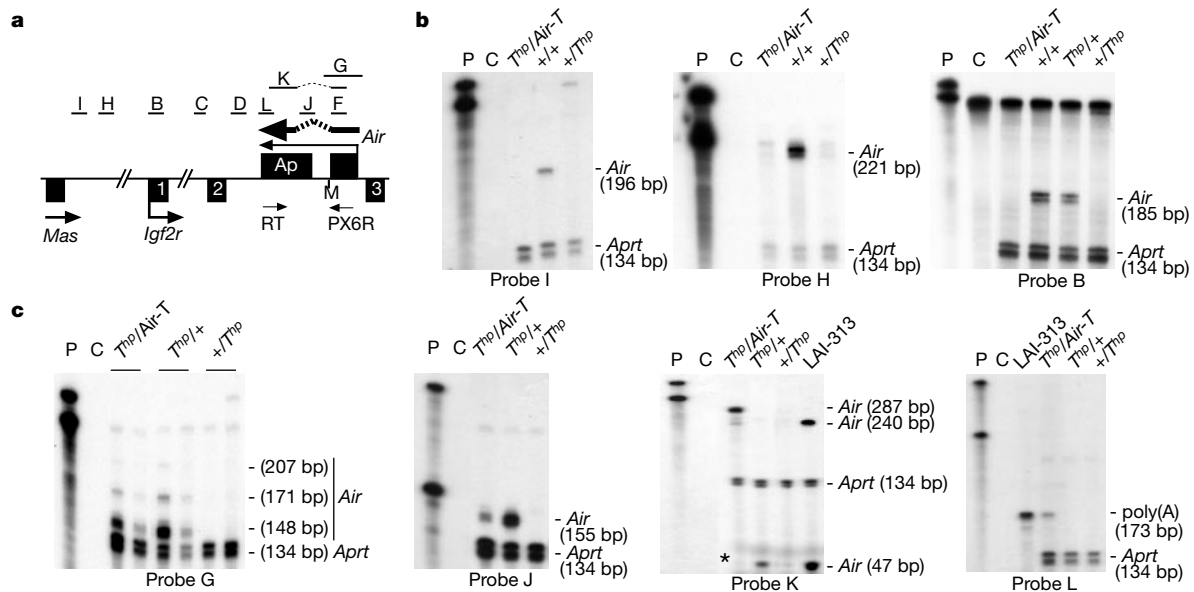


Figure 2 The *Air-T* allele truncates the *Air* RNA. **a**, Position of RNA probes (B–D, F–J, K (intron spanning), L), and RT and PX6R oligonucleotides used in RT-PCR, relative to those of *Mas*, *Igf2r* (exons 1–3) and *Air* on the *Air-T* allele. Unspliced *Air-T*, thin arrow; spliced *Air-T*, dashed arrow; *Air-T* exon 1, black box upstream from the *MluI* (M) site; polyadenylation cassette, Ap. **b**, RPA with probes B (on 11.5-d.p.c. embryo RNA), H and I (on adult heart RNA) indicates the absence of *Air* at, respectively, 28, 41 and 95 kb downstream from Ap. Identical results were obtained with probes C and D (Supplementary Information). **c**, RPA with probes G and J–L on 11.5-d.p.c. embryo RNA shows expression of truncated spliced and unspliced *Air-T* RNA. Probe G (which overlaps a +53-bp splice donor and multiple *Air* transcription start sites) protects 207, 171 and 148 bp of unspliced *Air* RNA from the *Air-T* paternal allele. However, the signal quantified by phosphorimager was reduced by 80% compared with that of the wild-type paternal allele (note the relative loading of *Air-T* and *T^{hp}/+* and that spliced fragments

protected by probe G are not visible). The signal reduction for unspliced *Air-T* is confirmed by probe J (which is located in the intron of the spliced *Air-T* RNA). Probe K is an RT-PCR fragment generated with oligonucleotides RT and PX6R (Supplementary Information) and protects 287 bp of spliced and 240 bp plus 47 bp of unspliced *Air-T* RNA (the 240-bp fragment is specific for the Ap cassette; asterisk indicates a faint 47-bp *Air* fragment). Probe K shows a ratio of 80% spliced and 20% unspliced *Air-T* RNA. The multicopy transgene LAI-313 contains the identical polyadenylation cassette¹⁴, and more clearly protects the 240- and 47-bp unspliced *Air* fragments. Probe L spans the AATAAA polyadenylation signal and protects 173 bp of *T^{hp}/Air-T* and LAI-313. The absence of larger, protected probe-L fragments confirms that both the spliced and unspliced *Air-T* RNAs are truncated at the polyadenylation signal. In **b** and **c**, parental alleles are denoted maternal/paternal, the loading control is *Aprt* exon 3, input probes are indicated by P, and the tRNA control by C.

observation that the *Air-T* promoter was expressed and imprinted in a similar manner to that of the *Air* wild-type promoter indicates that function of the 3.7-kb ICE was not disturbed.

We examined the effect of the truncated *Air-T* RNA on paternal silencing of the imprinted cluster. Of the three genes in this cluster, only *Igf2r* becomes methylated when silenced on the wild-type paternal allele⁵. Methylation of *Igf2r* is completely absent from the paternal *Air-T* allele in contrast to the wild-type allele (Fig. 4a). We used RNA blots to assess imprinted expression and show (Fig. 4b, c) that all three genes, *Igf2r*, *Slc22a2* and *Slc22a3*, have a complete loss of silencing on the paternal *Air-T* allele. Maternal expression of all three genes from the *Air-T* allele was at the same level as maternal expression from the wild-type allele, indicating that the targeting event did not alter their expression.

The *Air-T* allele truncated the *Air* RNA to 4% of its length yet maintained the imprinted status and expression level of the wild-type paternal *Air* promoter (with the caveats noted above). This truncation caused a complete loss of silencing of the *Igf2r/Slc22a2/Slc22a3* cluster on the paternal chromosome. This shows that the *Air* non-coding RNA is required for *cis* repression of flanking protein-coding genes. The identification of a role for the *Air* non-coding RNA in *cis* repression contrasts with the previous observation that DNA insulator and silencer elements regulate imprinting of the *Ins2/Igf2/H19* cluster^{10–12}. Our results thus identify a new RNA-dependent mechanism in genomic imprinting.

The bidirectional action of the *Air* RNA shown by our data is unexpected because the wild-type *Air* RNA overlaps only one gene.

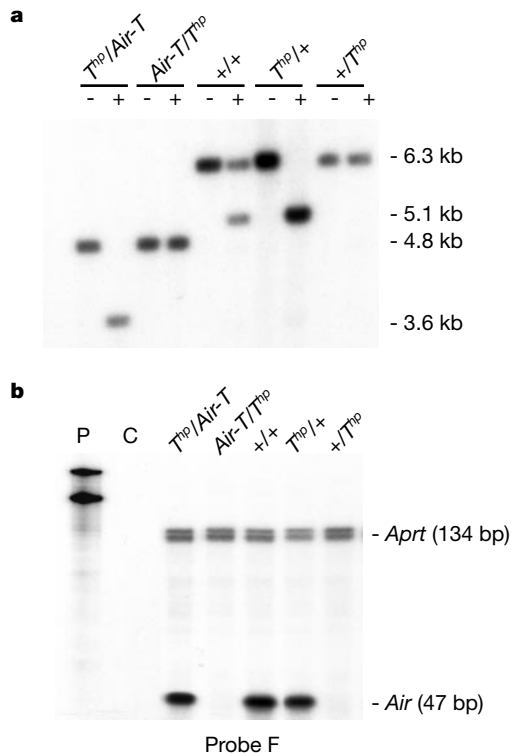


Figure 3 The *Air-T* allele is imprinted. **a**, The *Air-T* allele retains a methylation imprint on the *Air* promoter. DNA from 11.5-d.p.c. embryos cut with *EcoRI* (-) or *EcoRI/MluI* (+) was analysed with probe E. The fragments correspond to wild type methylated, 6.3 kb; wild type unmethylated, 5.1 kb; *Air-T* methylated, 4.8 kb; and *Air-T* unmethylated, 3.6 kb. Identical results were obtained with adult tail and spleen, and *SfuI* (Supplementary Information). **b**, The *Air-T* allele maintains imprinted *Air* expression. RPA was carried out on 11.5-d.p.c. embryo RNA with probe F, which detects spliced and unspliced *Air*. The paternal *Air-T* and wild-type alleles show equal *Air* expression, whereas the maternal alleles repress *Air*. Identical results were obtained with heart RNA and probes G, J and K (Supplementary Information). P, input probes; C, tRNA control.

Repression, at least of *Slc22a2* and *Slc22a3*, does not require transcriptional overlap, yet overlap with non-coding RNAs has been found at five independent imprinted loci^{3,15–18}. It is possible that the transcriptional overlap by non-coding RNAs may be involved if silencing of the non-overlapped genes were secondary to silencing of the overlapped gene. In this two-step model, the antisense non-coding RNA might repress the overlapped promoter (for example, by promoter occlusion or a form of *cis*-acting RNA interference; note that expression–competition³ is excluded by our findings) and induce a silent chromatin state that could spread bidirectionally in a limited manner and silence flanking genes.

Alternatively, if transcriptional overlap is not involved in *cis* repression, then the non-coding RNAs might function to recruit repressor proteins to the gene cluster. This latter model has parallels with X inactivation in female mammals, in which expression of the non-coding *Xist* RNA inactivates one X chromosome in *cis*¹⁹. The *Xist* RNA has features that have not been characterized as yet or that might be absent from imprinted non-coding RNAs, such as the ability to coat and spread along the length of the repressed chromosome^{20–23}. Although further testing is clearly necessary to determine whether there are mechanistic similarities at the molecular level, it is notable that X inactivation has been suggested to have evolved from a localized form of imprinting that initially

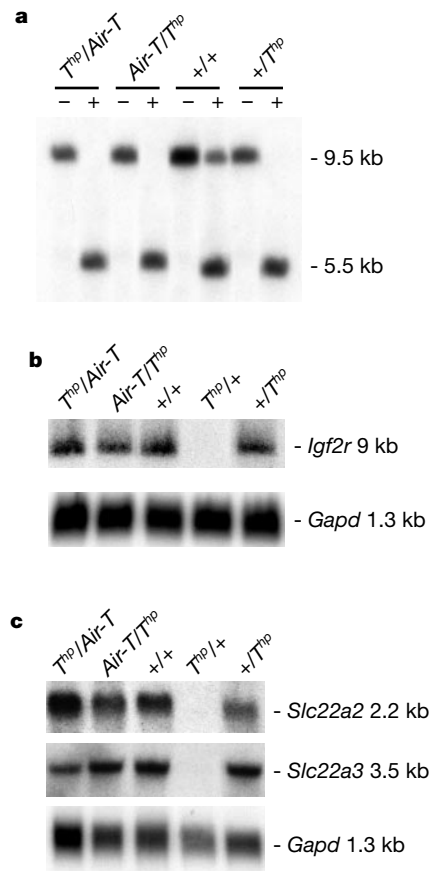


Figure 4 Loss of paternal silencing on the *Air-T* allele. **a**, The *Igf2r* promoter on the *Air-T* allele lacks paternal methylation. Tail DNA was cut with *BglII* (-) or *BglII/SalI* (+) and analysed with probe A. Methylated fragment, 9.5 kb; unmethylated fragment, 5.5 kb. Identical results were obtained with adult spleen DNA and either *NotI* or *SmaI* (Supplementary Information). **b**, Loss of paternal *Igf2r* repression on the *Air-T* allele. RNA from 11.5-d.p.c. embryos was analysed with a probe covering exons 3–6 from *Igf2r*. Identical results were obtained with adult heart RNA (Supplementary Information). **c**, Loss of paternal *Slc22a2* and *Slc22a3* repression on the *Air-T* allele. RNA from 11.5-d.p.c. placenta was analysed with cDNA probes for *Slc22a2* and *Slc22a3*. In **b** and **c**, *Gapd* is a control for RNA loading.

affected only a small region of the X chromosome that contains a dosage-sensitive gene^{24,25}. □

Methods

Generation of the *Air-T* allele

The targeting vector was constructed from a 9.6-kb *Bgl*II fragment (bp 117,878–127,575; AJ249895). A selection cassette containing *neomycin* and the thymidine kinase gene, each driven by a PGK promoter flanked by loxP sites plus a 1.2-kb fragment from the rabbit β -globin gene (bp 31,392–32,590; M18818) containing part of exon 2, complete intron 3 and complete exon 3 with the polyadenylation signal in the correct orientation for the *Air* promoter, was inserted at the *Bam*HI site in this fragment. The selection cassette was deleted by electroporation of a plasmid encoding Cre recombinase²⁶ and transient puromycin selection. We generated chimaeric mice by injecting paternally targeted *Air-T* embryonic stem (ES) cells into C57/Bl6 blastocysts²⁷. Mice carrying the *Air-T* allele were maintained on an FVB/N background.

Methylation and expression analyses

Digestion of methyl-sensitive enzymes was monitored by hybridization to mitochondrial DNA. We carried out RPA using an RPAIII kit (Ambion). Signals were quantified with a Phosphorimager (Fujix). For RT-PCR, 5 μ g heart RNA was reverse transcribed with Superscript (Gibco) using the linker-poly(dT) primer RT, 5'-CTGGGAAACAGCTATGACCATGATCGATTTTTTTTTTTTTTTT-3', and amplified with PX6R, 5'-GAAGCACAGCACCAGTAC-3', for 30 cycles (94 °C, 30 s; 59 °C, 30 s; 72 °C, 120 s).

Probes for DNA analyses

We used the following probes: probe A, a 325-bp PCR fragment (bp 102,813–103,137; AJ249895); probe C, a 0.9-kb *Eco*RI/*Hin*CII fragment from EST AA592338 (ref. 6) collinear with genomic DNA; probe D, (bp 121,834–122,862; AJ249895); and probe E (bp 124,992–126,086; AJ249895).

Probes for RNA analyses

Probe B, described as probe GFP^{PAIR}¹⁴, is 322 bp and protects 185 bp of *Air* RNA at the *Igf2r* promoter. Probes C and D are the same as the DNA analyses probes. Probe F is 174 bp and protects 47 bp (bp 126,181–126,227; AJ249895) immediately downstream from the principal *Air* transcription start site⁶. Probe G (bp 126,086–126,293; AJ249895), described as probe MIMs1 (refs 6,14), detects unspliced (207, 171 and 148 bp) *Air* RNA fragments. This relatively large probe did not produce a clear signal for the spliced *Air-T* RNA (predicted fragments of 112, 76 and 53 bp), which should have been recognized (see probe K below). Probe H, described as probe RPA1 (ref. 6), protects 221 bp of *Air* RNA (bp 85,250–85,029; AJ249895). Probe I, described as probe MS1B8 (ref. 6) protects 196 bp. Probe J is 173 bp and protects 155 bp of *Air* RNA (bp 123,233–123,387; AJ249895). Probe K is 364 bp, contains the RT-PCR fragment made with probes RT and PX6R (Supplementary Information) and protects 287 bp of spliced and 240 and 47 bp of unspliced polyadenylated RNA. Probe L spans 558 bp (bp 32,032–32,590; M18818) of the β -globin gene (including the polyadenylation signal) and protects 173 bp of polyadenylated RNA (bp 32,032–32,204; M18818). Probe L extends 385 bp downstream from the polyadenylation signal and the absence of protected fragments longer than 173 bp indicates use of the polyadenylation signal. The *Aprt* template is a 252-bp *Xho*I/*Xba*I fragment (bp 2,165–2,417; M11310) and protects *Aprt* exon 3 (134 bp). For RNA blots, we used the following probes: for *Igf2r*, complementary DNA exons 3–6; for *Slc22a2*, bp 989–1,605 (AJ006036); for *Slc22a3* bp 1–2,766 (AF078750); for *Gapd*, complete cDNA.

Received 27 September; accepted 4 December 2001.

1. Reik, W. & Walter, J. Genomic imprinting: parental influence on the genome. *Nature Rev. Genet.* **2**, 21–32 (2001).
2. Sleutels, F. & Barlow, D. P. in *Homology Effects* (eds Wu, C.-t. & Dunlap, C.) (Academic, San Diego, in the press).
3. Wutz, A. *et al.* Imprinted expression of the *Igf2r* gene depends on an intronic CpG island. *Nature* **389**, 745–749 (1997).
4. Wutz, A. *et al.* Non-imprinted *Igf2r* expression decreases growth and rescues the *Tme* mutation in mice. *Development* **128**, 1881–1887 (2001).
5. Zwart, R., Sleutels, F., Wutz, A., Schinkel, A. H. & Barlow, D. P. Bidirectional action of the *Igf2r* imprint control element on upstream and downstream imprinted genes. *Genes Dev.* **15**, 2361–2366 (2001).
6. Lyle, R. *et al.* The imprinted antisense RNA at the *Igf2r* locus overlaps but does not imprint *Mas1*. *Nature Genet.* **25**, 19–21 (2000).
7. Beechey, C. V., Cattanach, B. M. & Selley, R. L. Mouse Imprinting Data and References. *MRC Mammalian Genetics Unit* [online] (<http://www.mgu.har.mrc.ac.uk/imprinting/imprinting.html>) (2000).
8. Schmidt, J. V., Levorso, J. M. & Tilgham, S. M. Enhancer competition between H19 and *Igf2* does not mediate their imprinting. *Proc. Natl Acad. Sci. USA* **96**, 9733–9738 (1999).
9. Hark, A. T. *et al.* CTCF mediates methylation-sensitive enhancer-blocking activity at the H19/*Igf2* locus. *Nature* **405**, 486–489 (2000).
10. Constancia, M. *et al.* Deletion of a silencer element in *Igf2* results in loss of imprinting independent of H19. *Nature Genet.* **26**, 203–206 (2000).
11. Bell, A. C. & Felsenfeld, G. Methylation of a CTCF-dependent boundary controls imprinted expression of the *Igf2* gene. *Nature* **405**, 482–485 (2000).
12. Reik, W. & Murrell, A. Genomic imprinting. Silence across the border. *Nature* **405**, 408–409 (2000).
13. Wang, Z. Q., Fun, M. R., Barlow, D. P. & Wagner, E. F. Regulation of embryonic growth and lysosomal targeting by the imprinted *Igf2/Mpr* gene. *Nature* **372**, 464–467 (1994).
14. Sleutels, F. & Barlow, D. P. Investigation of elements sufficient to imprint the mouse *Air* promoter. *Mol. Cell. Biol.* **21**, 5008–5017. (2001).

15. Wroe, S. F. *et al.* An imprinted transcript, antisense to *Nesp*, adds complexity to the cluster of imprinted genes at the mouse *Gnas* locus. *Proc. Natl Acad. Sci. USA* **97**, 3342–3346 (2000).
16. Lee, Y. J. *et al.* *Mit1/Lb9* and *Copg2*, new members of mouse imprinted genes closely linked to *Peg1/Mest1*. *FEBS Lett.* **472**, 230–234 (2000).
17. Rougeulle, C., Cardoso, C., Fontes, M., Colleaux, L. & Lalande, M. An imprinted antisense RNA overlaps *UBE3A* and a second maternally expressed transcript. *Nature Genet.* **19**, 15–16 (1998).
18. Smilnich, N. J. *et al.* A maternally methylated CpG island in *KvLQT1* is associated with an antisense paternal transcript and loss of imprinting in Beckwith-Wiedemann syndrome. *Proc. Natl Acad. Sci. USA* **96**, 8064–8069 (1999).
19. Avner, P. & Heard, E. X-chromosome inactivation: counting, choice and initiation. *Nature Rev. Genet.* **2**, 59–67 (2001).
20. Clemson, C. M., McNeil, J. A., Willard, H. F. & Lawrence, J. B. XIST RNA paints the inactive X chromosome at interphase: evidence for a novel RNA involved in nuclear/chromosome structure. *J. Cell Biol.* **132**, 259–275 (1996).
21. Lee, J. T., Strauss, W. M., Dausman, J. A. & Jaenisch, R. A 450 kb transgene displays properties of the mammalian X-inactivation center. *Cell* **86**, 83–94 (1996).
22. Sheardown, S. A. *et al.* Stabilization of *Xist* RNA mediates initiation of X chromosome inactivation. *Cell* **91**, 99–107 (1997).
23. Wutz, A. & Jaenisch, R. A shift from reversible to irreversible X inactivation is triggered during ES cell differentiation. *Mol. Cell* **5**, 695–705 (2000).
24. Lyon, M. F. Imprinting and X-chromosome inactivation. *Results Probl. Cell Differ.* **25**, 73–90 (1999).
25. Graves, J. A. Mammals that break the rules: genetics of marsupials and monotremes. *Annu. Rev. Genet.* **30**, 233–260 (1996).
26. O’Gorman, S., Dagenais, N. A., Qian, M. & Marchuk, Y. Protamine-Cre recombinase transgenes efficiently recombine target sequences in the male germ line of mice, but not in embryonic stem cells. *Proc. Natl Acad. Sci. USA* **94**, 14602–14607 (1997).
27. Hogan, B. L. M., Beddington, R. S. P., Costantini, F. & Lacy, E. *Manipulating the Mouse Embryo* (Cold Spring Harbor Laboratory Press, Cold Spring Harbor, 1994).

Supplementary Information accompanies the paper on *Nature’s* website (<http://www.nature.com>).

Acknowledgements

We thank K. van Veen, K. van het Wout, P. Krimpenfort for help in generating mice; S. Greven, T. Maidment and N. Bosnic for care of the mice; A. Berns, H. te Riele, M. van Lohuizen, R. Beijersbergen, P. Borst and A. Frischauf for comments; and A. Berns for help and encouragement. This research was supported by the Dutch Cancer Society (KWF).

Correspondence and requests for materials should be addressed to D.P.B. (e-mail: dbarlow@imb.oeaw.ac.at).

Structural basis for antagonist-mediated recruitment of nuclear co-repressors by PPAR α

H. Eric Xu, Thomas B. Stanley, Valerie G. Montana, Millard H. Lambert, Barry G. Shearer, Jeffery E. Cobb, David D. McKee, Cristin M. Galardi, Kelli D. Plunket, Robert T. Nolte, Derek J. Parks, John T. Moore, Steven A. Kliewer, Timothy M. Willson & Julie B. Stimmel

Nuclear Receptor Discovery Research, GlaxoSmithKline, Research Triangle Park, North Carolina 27709, USA

Repression of gene transcription by nuclear receptors is mediated by interactions with co-repressor proteins such as SMRT and N-CoR^{1,2}, which in turn recruit histone deacetylases to the chromatin^{3–5}. Aberrant interactions between nuclear receptors and co-repressors contribute towards acute promyelocytic leukaemia and thyroid hormone resistance syndrome^{6–8}. The binding of co-repressors to nuclear receptors occurs in the unliganded state, and can be stabilized by antagonists⁹. Here we report the crystal structure of a ternary complex containing the peroxisome proliferator-activated receptor- α ligand-binding domain bound to the antagonist GW6471 and a SMRT co-repressor motif. In this structure, the co-repressor motif adopts a three-turn α -helix that prevents the carboxy-terminal activation helix (AF-2) of the receptor from assuming the active conformation. Binding of